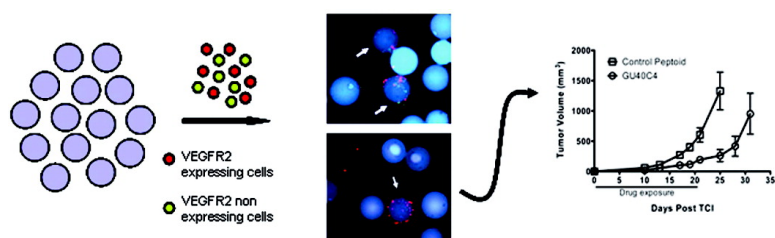


A Peptoid “Antibody Surrogate” That Antagonizes VEGF Receptor 2 Activity

D. Gomika Udugamasooriya, Sean P. Dineen, Rolf A. Brekken, and Thomas Kodadek

J. Am. Chem. Soc., **2008**, 130 (17), 5744-5752 • DOI: 10.1021/ja711193x • Publication Date (Web): 02 April 2008

Downloaded from <http://pubs.acs.org> on February 8, 2009



More About This Article

Additional resources and features associated with this article are available within the HTML version:

- Supporting Information
- Links to the 3 articles that cite this article, as of the time of this article download
- Access to high resolution figures
- Links to articles and content related to this article
- Copyright permission to reproduce figures and/or text from this article

[View the Full Text HTML](#)

A Peptoid “Antibody Surrogate” That Antagonizes VEGF Receptor 2 Activity

D. Gomika Udugamasooriya,[†] Sean P. Dineen,^{‡,§,¶} Rolf A. Brekken,^{‡,§,¶} and Thomas Kodadek^{*,†,⊥}

Division of Translational Research, Departments of Internal Medicine, Surgery, and Pharmacology, and Hamon Center for Therapeutic Oncology Research and Molecular Biology, University of Texas Southwestern Medical Center, 5323 Harry Hines Boulevard, Dallas, Texas 75390-9185

Received December 17, 2007; E-mail: thomas.kodadek@utsouthwestern.edu

Abstract: We report a two-color, cell-based screen to identify specific receptor-binding compounds in a combinatorial library of peptoids displayed on beads. We apply this strategy to the isolation of vascular endothelial growth factor receptor 2 (VEGFR2)-binding peptoids. A dimeric derivative of one of these lead compounds is shown to be an antagonist of VEGFR2 activity both in vitro and in vivo. This methodology provides a potentially general route to synthetic molecules that bind integral membrane receptors with affinities and specificities similar to those of antibodies, but which are far smaller and easier to make and manipulate.

Introduction

Monoclonal antibodies are used widely in the clinic. Most function by binding to hormones or the extracellular domains of integral membrane proteins and thus antagonizing their function.^{1,2} In addition, antibody conjugates are employed to deliver toxic cargo to cells that express a particular receptor.³ However, therapeutic antibodies have significant limitations. They are difficult and expensive to manufacture. Their large size (~150 kD) results in a low “cargo-carrying capacity” on a mass/mass basis, limited tumor penetration,⁴ and can induce an immune reaction⁵ unless the antibody is fully humanized.⁶ Therefore, it is of great interest to develop much smaller, synthetic compounds that display antibody-like affinity and specificity, but which could be made cheaply and be easily tailored to carry cargo of various sorts. Unfortunately, it has proven difficult to isolate small molecules, other than peptides,⁷ that bind with high affinity to large, shallow interaction surfaces, such as those present on the extracellular surface of integral membrane receptors.⁸ In a few cases, peptide antagonists have been developed into clinically useful compounds,⁹ but this

approach to drug development is limited severely by the sensitivity of peptides to proteolysis. While there are many examples of other small molecular antagonists of receptors, these generally function by alternative mechanisms, for example, as inhibitors of ligand-activated kinase activity.¹⁰

We report here a potentially general solution to this problem using an alternative approach. We and others have demonstrated that libraries of peptoids (oligo-N-substituted glycines) are rich sources of protein-binding ligands.^{11,12} Unlike peptides, peptoids are not sensitive to peptidases or proteases¹³ and are even easier and more economical to synthesize than peptides¹⁴ (Supplementary Figure 1). Using vascular endothelial growth factor receptor 2 (VEGFR2) as a target, we describe a novel two-color, cell-based screen that allows large peptoid libraries to be screened for receptor-binding compounds. The “hits” bind VEGFR2 with dissociation constants (K_D) in the low micromolar region and can be modified easily through dimerization to create low nanomolar VEGFR2 ligands. We show that one of these dimeric peptoids functions as an antagonist of VEGFR2 activation in vitro and angiogenesis and tumor growth in vivo.

Results

A Two-Color, Cell-Based Binding Screen for VEGFR2-Binding Peptoids. Peptoid (oligo-N-alkylglycines) libraries have been shown to be an excellent source of protein-binding

[†] Department of Internal Medicine.
[‡] Department of Molecular Biology.
[§] Department of Surgery.
[¶] Department of Pharmacology.
[⊥] Hamon Center for Therapeutic Oncology Research and Molecular Biology.

(1) Gerber, H. P.; Ferrara, N. *Cancer Res.* **2005**, *65*, 671–680.
(2) Taylor, P. C. *Intern. Med.* **2003**, *42*, 15–20.
(3) Segota, E.; Bukowski, R. M. *Cleve. Clin. J. Med.* **2004**, *71*, 551–560.
(4) Aina, O. H.; Sroka, T. C.; Chen, M. L.; Lam, K. S. *Biopolymers* **2002**, *66*, 184–199.
(5) Stevenson, G. T. *Leuk. Res.* **2005**, *29*, 239–246.
(6) Mateo, C.; Lombardero, J.; Moreno, E.; Morales, A.; Bombino, G.; Coloma, J.; Wims, L.; Morrison, S. L.; Perez, R. *Hybridoma* **2000**, *19*, 463–471.
(7) D’Andrea, L. D.; Del Gatto, A.; Pedone, C.; Benedetti, E. *Chem. Biol. Drug Des.* **2006**, *67*, 115–126.
(8) Whitty, A.; Kumaravel, G. *Nat. Chem. Biol.* **2006**, *2*, 112–118.

(9) Liu, S.; Wu, S.; Jiang, S. *Curr. Pharm. Des.* **2007**, *13*, 143–162.
(10) Ciardiello, F.; De Vita, F.; Orditura, M.; De Placido, S.; Tortora, G. *Exp. Opin. Emerg. Drugs* **2003**, *8*, 501–514.
(11) Alluri, P. G.; Reddy, M. M.; Bachhawat-Sikder, K.; Olivos, H. J.; Kodadek, T. *J. Am. Chem. Soc.* **2003**, *125*, 13995–14004.
(12) Zuckermann, R. N.; Martin, E. J.; Spellmeyer, D. C.; Stauber, G. B.; Shoemaker, K. R.; Kerr, J. M.; Figliozzi, G. M.; Goff, D. A.; Siani, M. A.; Simon, R. J.; al, e. *J. Med. Chem.* **1994**, *37*, 2678–2685.
(13) Simon, R. J.; Kania, R. S.; Zuckermann, R. N.; Huebner, V. D.; Jewell, D. A.; Banville, S.; Ng, S.; Wang, L.; Rosenberg, S.; Marlowe, C. K.; Spellmeyer, D. C.; Tan, R.; Frankel, A. D.; Santi, D. V.; Cohen, F. E.; Bartlett, P. A. *Proc. Natl. Acad. Sci. U.S.A.* **1992**, *89*, 9367–9371.

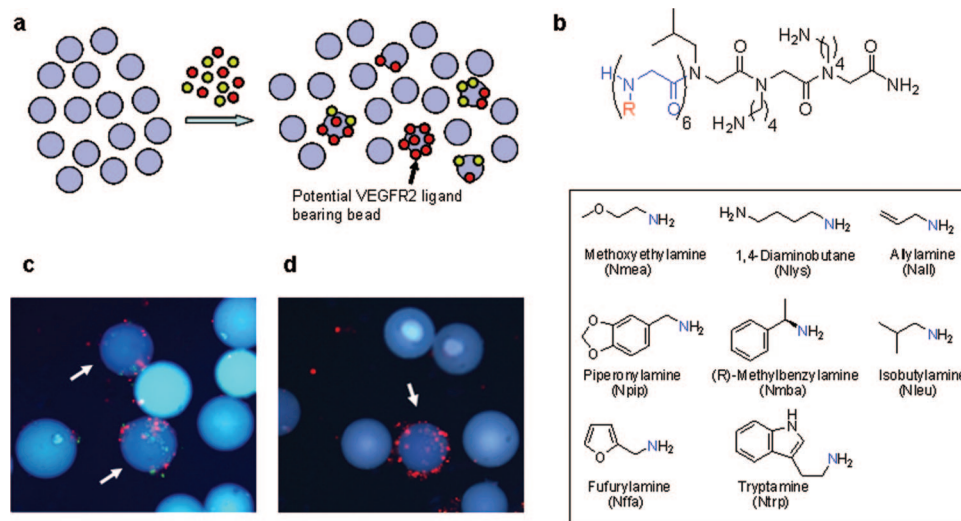


Figure 1. A two-color, cell-based assay for the identification of peptoid ligands for VEGFR2. (a) Schematic representation of the assay. The large blue circles represent peptoid library beads, and the small red and green circles represent quantum-dot-stained PAE/KDR (VEGFR2 overexpressing) cells and PAE parental (lacking VEGFR2) cells, respectively. Beads that display peptoids that bind specifically to VEGFR2 should retain only red-stained cells. (b) Structure of the peptoid library employed in the screen. Top: general structure of the compounds in the library. Three residues at the C-terminus were fixed, and the remaining six residues (drawn in blue) were diversified (side chains represented by "R", drawn in red). Box: the amines employed to make the library. The nitrogen shown in blue becomes the main chain nitrogen in the peptoid. (c) and (d) Fluorescence microscopic images of select beads after screening and washing ($100\times$ total magnification; DAPI filter). The arrows in (c) indicate beads that bind both cells that do and do not express VEGFR2. The bead indicated by the arrow in (d) represents one of five out of $\sim 300\,000$ observed to bind only red-stained cells.

compounds with affinities comparable to those exhibited by peptide ligands,^{11,15–18} but with far superior pharmacokinetic properties.¹⁹ To screen bead-displayed peptoid libraries against integral cell membrane protein targets, specifically VEGFR2 in this case, we developed the assay shown schematically in Figure 1a. Porcine aortic endothelial (PAE) cells lacking human VEGFR2 were labeled with green-emitting quantum dots, and PAE cells expressing human VEGFR2 (PAE/KDR) were labeled with red-emitting quantum dots. These cells, which, in theory, differ only in the presence of the VEGFR2, were then mixed in an approximately 1:1 ratio and exposed to the bead-displayed peptoid library of over 250 000 compounds with the general structure shown in Figure 1b. After thorough washing, the beads were examined under a fluorescence microscope (excitation at 340–380 nm through a standard DAPI filter), allowing simultaneous visualization of the beads, which fluoresce blue, and both cell types, which fluoresce green and red, respectively (Figure 1c,d). As expected, the vast majority of the beads did not bind either cell type. A much smaller number of beads were observed to bind both the red- and green-stained cells (large blue sphere with both green and red speckles indicated with the arrow in Figure 1c). Only five of the approximately 300 000 beads screened (approximately 0.0017% of the population) were observed to bind only red PAE/KDR cells (see Figure 1d). These putative "hits" were collected using a micropipette, and the

sequences of the peptoids were determined by Edman degradation (Figure 2 and Supplementary Figure 2).

The Isolated Peptoids are VEGFR2 Ligands. Two of the hits from this screen, GU40C and GU40E (Figure 2a), as well as fluoresceinated derivatives, were resynthesized and purified. Their association with VEGFR2 was evaluated using an ELISA-like assay. A protein containing the extracellular domain of human VEGFR2 fused to human Fc was coated onto 96-well plates and incubated with various concentrations of FITC-labeled peptoid. As shown in Figure 2b and Supplementary Table 1, the peptoids bound to VEGFR2 with K_D values of about $2\ \mu\text{M}$. These values are similar to²⁰ or better than^{21,22} those reported previously for VEGFR2-binding peptides. GU40C and GU40E did not bind detectably to another endothelial cell surface receptor, CD105 or to GST, in the same assay (Figure 2b). Conversely, a peptoid (see Supplementary Figure 3) not selected to bind VEGFR2 did not compete with GU40C or GU40E for binding to VEGFR2 (Figure 2c). Self-competition between the fluoresceinated and unlabeled forms of GU40C and GU40E confirmed that the fluorescent label was not important for the observed binding to VEGFR2 (Figure 2c).

Functional Characterization of the Monomeric VEGFR2-Binding Peptoids. GU40C and GU40E were tested for their ability to modulate VEGFR2 function. An early step in the angiogenesis cascade is autophosphorylation of the kinase domain of VEGFR2 upon VEGF binding. We incubated PAE/KDR cells with or without 1.3 nM (50 ng/mL) VEGF and/or several different concentrations of the peptoid ligands. Phos-

(14) Zuckermann, R. N.; Kerr, J. M.; Kent, S. B. H.; Moos, W. H. *J. Am. Chem. Soc.* **1992**, *114*, 10646–10647.

(15) Alluri, P. G.; Liu, B.; P., Y.; Xiao, X.; Kodadek, T. *Mol. BioSyst.* **2006**, *2*, 568–579.

(16) Bachhawat-Sikder, K.; Kodadek, T. *J. Am. Chem. Soc.* **2003**, *125*, 9550–9551.

(17) Liu, B.; Alluri, P. G.; Yu, P.; Kodadek, T. *J. Am. Chem. Soc.* **2005**, *127*, 8254–8255.

(18) Reddy, M. M.; Bachhawat-Sikder, K.; Kodadek, T. *Chem. Biol.* **2004**, *11*, 1127–1137.

(19) Simon, R. J.; Kania, R. S.; Zuckermann, R. N.; Huebner, V. D.; Jewell, D. A.; Banville, S.; Ng, S.; Wang, L.; Rosenberg, S.; Marlowe, C. K.; Spellmeyer, D. C.; Tan, R.; Frankel, A. D.; Santi, D. V.; Cohen, F. E.; Bartlett, P. A. *Proc. Natl. Acad. Sci. U.S.A.* **1992**, *89*, 9367–9371.

(20) Zilberberg, L.; Shinkaruk, S.; Lequin, O.; Rousseau, B.; Hagedorn, M.; Costa, F.; Caronzolo, D.; Balke, M.; Cannon, X.; Convert, O.; Lain, G.; Gionnet, K.; Goncalves, M.; Bayle, M.; Bello, L.; Chassaing, G.; Deleris, G.; Bikfalvi, A. *J. Biol. Chem.* **2003**, *278*, 35564–35573.

(21) Binetruy-Tournaire, R.; Demangel, C.; Malavaud, B.; Vassy, R.; Rouyre, S.; Kraemer, M.; Plouet, J.; Derbin, C.; Perret, G.; Mazie, J. C. *EMBO J.* **2000**, *19*, 1525–1533.

(22) Hetian, L.; Ping, A.; Shumei, S.; Xiaoying, L.; Luowen, H.; Jian, W.; Lin, M.; Meisheng, L.; Junshan, Y.; Chengchao, S. *J. Biol. Chem.* **2002**, *277*, 43137–43142.

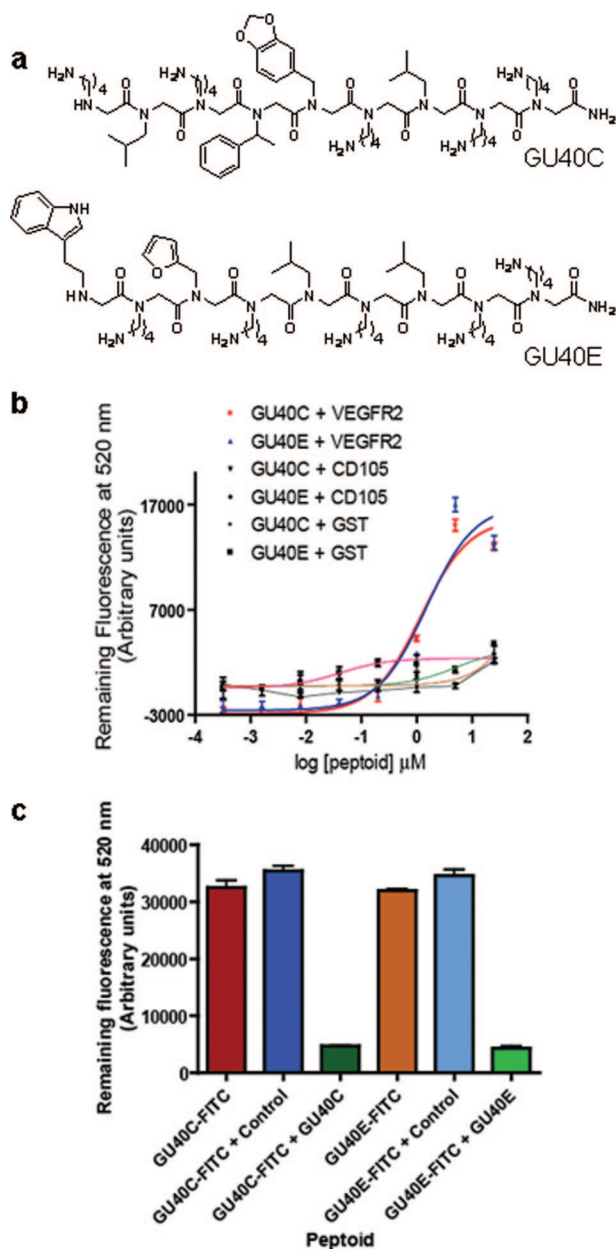


Figure 2. Two of the hits identified in the screen and their affinities for VEGFR2. (a) Chemical structures of two of the initial hits identified (GU40C and GU40E). (b) Binding isotherms of fluorescein-conjugated peptoids GU40C and GU40E against immobilized VEGFR2, CD105, and GST proteins evaluated by ELISA-like assay. (c) Binding competition of fluoresceinated GU40C and GU40E peptoids with unlabeled GU40C, GU40E, and control peptoid against VEGFR2 evaluated by ELISA-like assay. Both fluoresceinated peptoids were at $5 \mu\text{M}$, both unlabeled peptoids were at $25 \mu\text{M}$, and control peptoid was at $50 \mu\text{M}$.

phorylation of VEGFR2 was determined by Western blot analysis. As shown in Supplementary Figure 5, neither peptoid induced VEGFR2 phosphorylation. Instead, both GU40C and GU40E appeared to be weak antagonists of VEGF-dependent VEGFR2 autophosphorylation. At a peptoid concentration of $500 \mu\text{M}$, an approximately 75% inhibition of phosphorylation was observed (Supplementary Figure 6).

High Affinity Dimeric VEGFR2-Binding Peptoids. To transform the hit peptoids rapidly into high affinity lead compounds, we took advantage of the fact that VEGFR2, like many receptors, functions as a dimer. Indeed, while the K_D of the $(\text{VEGF})_2 \cdot (\text{VEGFR})_2$ complex is 50 pM , a monomeric derivative

of VEGF binds to the VEGFR2 receptor dimer with an affinity of only $1.5 \mu\text{M}$,²³ a value quite similar to that exhibited by the GU40C and GU40E peptoids. The approach of employing avidity effects to generate high affinity ligands for dimeric or higher-order protein targets is an old one and has been applied successfully to cell surface receptors previously.^{24–26} Therefore, we synthesized and characterized homodimeric derivatives of GU40C and GU40E (Figure 3a and Supplementary Table 1). Homodimerization was achieved with a central Lys linker from which branch additional linker arms that would separate the N-termini of each monomeric unit by approximately 45–85 Å (the VEGFR2 binding regions of the dimeric hormone are separated by approximately 70 Å)²⁷ if the linkers were in their fully extended conformation. This was accomplished by using linkers with different numbers and combinations of β -alanine and aminohexanoic acid units (Figure 3a and Supplementary Table 1, GU40C1–5 and GU40E1–5). In addition, shorter dimers were obtained for compound GU40C by avoiding the additional linker region and also by truncating the three fixed C-terminal residues one at a time (Figure 3a and Supplementary Table 1, GU40CA-C).

The binding of each of these dimeric peptoids to VEGFR2 was analyzed using the same ELISA-like method. As shown in Figure 3b and Supplementary Table 1, the best result was obtained with GU40C4, with 72 backbone atoms (Figure 3c), which bound VEGFR2 with an apparent K_D of 30 nM (Figure 3d), an improvement of about 90-fold relative to the monomeric parent compound. These binding data were further confirmed by a solution phase fluorescence polarization study using fluorescein-labeled GU40C4 and the soluble extracellular domain of VEGFR2, which indicated a K_D of 20 nM (Supplementary Figure 7). This low nanomolar dissociation constant is similar to that exhibited by some monoclonal antibodies that recognize VEGFR2.^{28,29} Therefore, GU40C4 was chosen for further study. Finally, further ELISA analysis revealed that GU40C4 binds to VEGFR1, which is highly homologous to VEGFR2, with a similar affinity (Supplementary Figures 8 and 9).

Specificity of the GU40C4–VEGFR2 Interaction on the Cell Surface. To evaluate the specificity of the peptoid–receptor interaction, biotinylated GU40C4 was mixed with live cells that do or do not express VEGFR2. Binding was visualized using streptavidin-conjugated red quantum dots. GU40C4 bound to PAE/KDR cells (Figure 4a) but not PAE parental cells (Figure 4d). Binding to PAE/KDR cells was competed by 100-fold excess unlabeled GU40C4 (Figure 4b), demonstrating that the observed interaction is not the result of interaction of the streptavidin–quantum dots with the PAE/KDR cells (Figure 4c). GU40C4 did not bind detectably to HeLa (which express EGF

- (23) Fuh, G.; Li, B.; Crowley, C.; Cunningham, B.; Wells, J. A. *J. Biol. Chem.* **1998**, *273*, 11197–11204.
- (24) Page, M. I.; Jencks, W. P. *Proc. Natl. Acad. Sci. U.S.A.* **1971**, *68*, 1678–1683.
- (25) Mezo, A. R.; McDonnell, K. A.; Tan Hehir, C. A.; Low, S. C.; Palombella, V. J.; Stattel, J. M.; Kamphaus, G. D.; Fraley, C.; Zhang, Y.; Dumont, J. A.; Bitonti, A. J. *Proc. Natl. Acad. Sci. U.S.A.* **2008**, in press.
- (26) Kaabe, B. H.; Harpoe, K.; Kastrop, J. S.; Sanz, A. C.; Pickering, D. S.; Metzler, B.; Clausen, R. P.; Gajhede, M.; Sauerberg, P.; Liljefors, T.; Madsen, U. *Chem. Biol.* **2007**, *14*, 1294–1303.
- (27) Wiesmann, C.; Fuh, G.; Christinger, H. W.; Eigenbrot, C.; Wells, J. A.; de Vos, A. M. *Cell* **1997**, *91*, 695–704.
- (28) Brekken, R. A.; Huang, X.; King, S. W.; Thorpe, P. E. *Cancer Res.* **1998**, *58*, 1952–1959.
- (29) Lu, D.; Jimenez, X.; Zhang, H.; Bohlen, P.; Witte, L.; Zhu, Z. *Int. J. Cancer* **2002**, *97*, 393–399.

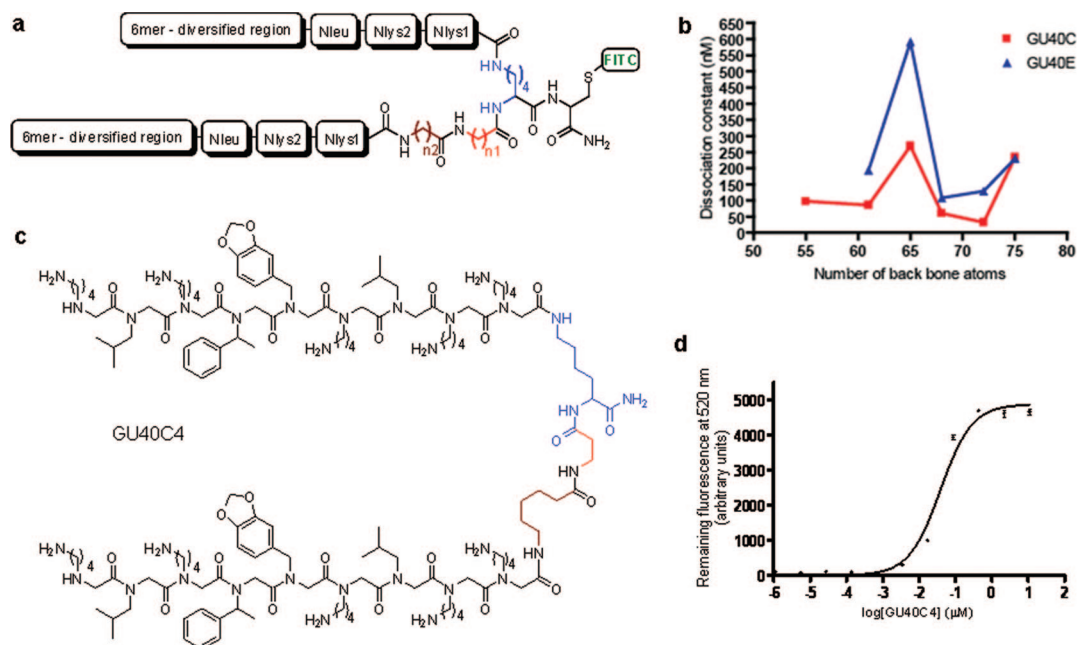


Figure 3. Dimeric peptoid design and evaluation of binding affinity. (a) General chemical structure of the dimeric compounds tested. Longer dimeric compounds (GU40C1–5 or GU40E1–5) contain two full monomeric units, connected by a Lys (blue) and variable number of β -alanine or γ -aminohexanoic acid linkers (red and brown; refer to Supplementary Table 1). The shorter dimers lack these linkers as well as one to three of the fixed residues at the C-terminus of each monomer unit (refer to Supplementary Table 1). Each compound was synthesized with a C-terminal Cys residue that was used to attach fluorescein via maleimide chemistry. (b) Binding affinities (shown as dissociation constants, K_D) for the two series of homodimeric peptoids derived from monomers GU40C (red) and GU40E (blue) as a function of the number of backbone atoms of the dimer. The best binding affinity was displayed by GU40C4 (72 backbone atoms). (c) Chemical structure of the best dimeric ligand identified, GU40C4. (d) Binding isotherm of fluoresceinated GU40C4 for immobilized human VEGFR2 extracellular domain ($K_D \approx 30$ nM).

receptors, but not VEGF receptors), HEK-293, or human foreskin fibroblast (HFF) cells but did bind to HUVEC, MCF-7, and PAE/Flt-1 cells (Figure 4e–j). Only HUVEC and MCF-7 cells express VEGFR2 (Figure 4f,g). PAE/Flt-1 cells express VEGFR1. Together, these data demonstrate that GU40C4 binds detectably to only VEGF receptors and does not associate with other cell surface molecules.

GU40C4 is an Antagonist of VEGF-Dependent Receptor Activation in vitro. To determine if peptoid GU40C4 is capable of modulating VEGFR2 function, we examined the effect of the peptoid on VEGF-induced VEGFR2 autophosphorylation in PAE/KDR as well as HUVEC. These experiments demonstrated that GU40C4 is an antagonist of receptor activation with an IC_{50} value of approximately $1 \mu\text{M}$ at a VEGF concentration of 1.3 nM (Figure 5a–d). This represents an improvement of between 100- and 500-fold over the monomeric parent compound (Supplementary Figures 5 and 6), consistent with the increased affinity of the dimeric peptoid. Under similar conditions, $1 \mu\text{M}$ Avastin, which binds VEGF, completely blocked VEGFR2 autophosphorylation (Figure 5a,c).

We also studied the ability of GU40C4 to inhibit hormone-induced proliferation of human vascular endothelial cells (HUVECs) treated with 1.3 nM VEGF. GU40C4 inhibited VEGF-induced HUVEC proliferation with an IC_{50} of approximately $1 \mu\text{M}$. At $10 \mu\text{M}$, the peptoid reduced cell proliferation to basal levels (Figure 5e). Ten micromolar FLAG peptide (Supplementary Figure 4), which was used as a negative control, did not have any affect on endothelial proliferation.

Finally, we examined the effect of GU40C4 on VEGF-induced endothelial tube formation (Supplementary Figures 10 and 11). HUVECs were seeded on a three-dimensional matrix in the presence of 1.3 nM VEGF and different concentrations of GU40C4 or various control compounds, including $10 \mu\text{M}$

control peptoid, GU40C (monomer), and GU40CC (ineffective shortest dimer; Supplementary Table 1). Clear evidence of the inhibition of tube formation could be seen at GU40C4 peptoid concentrations of 1 and $10 \mu\text{M}$ (Supplementary Figure 10, panels 4 and 5), while the control peptoid and GU40CC had no effect (Supplementary Figure 10, panels 6 and 8).

We conclude from these experiments that the dimeric peptoid GU40C4 is an antagonist of VEGF-induced VEGFR2 activity in vitro.

GU40C4 has in vivo Therapeutic Efficacy in a Preclinical Mouse Model. On the basis of the in vitro data shown above, we hypothesized that GU40C4 would inhibit tumor growth in a murine model. This was tested using A673 (human Ewing's sarcoma) cells implanted into the flank of athymic nude mice; $800 \mu\text{g}$ of GU40C4 ($n = 10$) or a control peptoid ($n = 11$) was delivered by an osmotic pump implanted subcutaneously at a site distant from the tumor on the day of tumor cell injection. The pumps eluted drug at a rate of $0.2 \mu\text{L/h}$ continuously for a period of 20.8 days. A third group of animals received only saline ($n = 6$). Tumor growth in the saline-treated animals did not differ from tumor growth in control peptoid treated animals (data not shown). Importantly, we observed no adverse effects of treatment with either GU40C4 or the control peptoid. Animals treated with GU40C4 had a reduced tumor growth rate and significantly smaller tumors at the end of therapy compared to control peptoid-treated animals (Figure 6a). Twenty-two days after tumor cell injection, five animals from each group were sacrificed for histological analysis (Figure 6b,c). We continued to follow the remaining animals for 10 days to determine the extent of tumor growth delay in the GU40C4-treated animals. Tumors remained small for approximately 1 week, suggesting that GU40C4 retained some effect after delivery had stopped. Histological analysis revealed that GU40C4 reduced microvessel

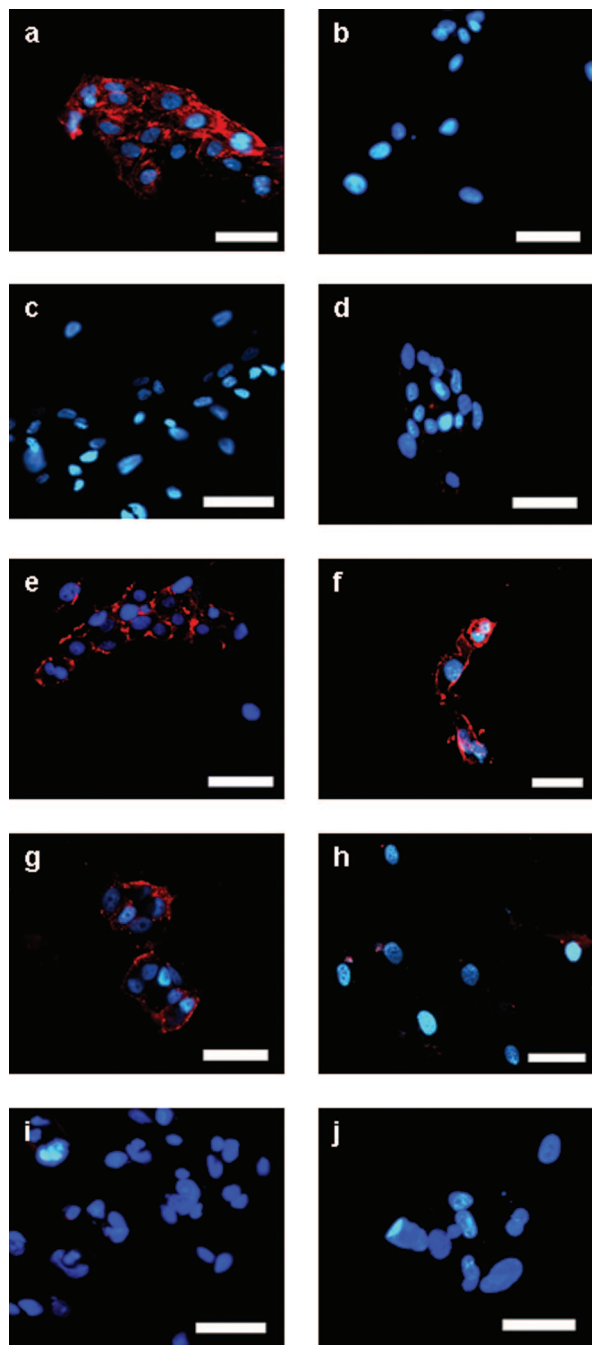


Figure 4. Cell-specific binding study for GU40C4. Live cells were treated with biotinylated GU40C4 and subsequently with streptavidin-conjugated red quantum dot as control (c), which was treated only with streptavidin-conjugated red quantum dot. The nuclei are stained with DAPI. Fluorescence microscopic images were taken under DAPI filter at 400 \times total magnification: (a) PAE/KDR cells, (b) PAE/KDR cells + 100-fold excess of unlabeled GU40C4, (c) PAE/KDR cells treated only with streptavidin-quantum dot, (d) PAE parental cells, (e) PAE/Flt-1 cells, (f) HUVEC, (g) MCF-7 cells, (h) HeLa cells, (i) HEK-293 cells, and (j) human foreskin fibroblasts (HFF). Of the cells shown in panels (e–j), only HUVEC and MCF-7 cells are known to express VEGFR2, and PAE/Flt-1 cells overexpress VEGFR1. GU40C4 binds to these cells only (images were taken using a DAPI filter at the same exposure and gain levels; the scale bar equals 50 μ m).

density by approximately 50% at day 22 post tumor cell injection ($p < 0.0001$, Figure 6b). Furthermore, GU40C4, but not the control peptoid, induced significant tumor necrosis as evaluated by H&E histology (Figure 6c). These data are

consistent with GU40C4-mediated inhibition of VEGF-induced angiogenesis in vivo and further validate our in vitro studies.

Discussion

Many hormone–receptor interactions have been identified as therapeutic targets. The VEGF–VEGFR2 complex, in particular, has received much attention for the treatment of certain cancers^{30,31} as well as “wet” macular degeneration,³² given its essential role in angiogenesis. The majority of VEGF pathway inhibitors reported to date are either monoclonal antibodies,^{33–35} other protein-based molecules,³⁶ or peptides⁷ targeting VEGF itself or the extracellular domain of one of the VEGF receptors. However, therapeutic antibodies typically display limited tumor penetration and are difficult and costly to manufacture in large quantities. More classical small molecules such as Sutent (Sunitinib, Pfizer),³⁷ Nexavar (Sorafenib, Bayer/Onyx),³⁸ and a few other small molecular VEGF receptor tyrosine kinase (RTK)-targeted drugs have also been approved for antiangiogenic therapy. However, due to the structural homology of many different kinase domains, most of these inhibitors show cross-reactivity with multiple receptors.³⁹ Finally, there are several reports of VEGF- and VEGFR2-binding peptides, but these molecules lack the affinity and serum stability to be of practical utility.

In this report, we examine peptoids as potential antibody surrogates. Large combinatorial libraries of peptoids can be synthesized easily and inexpensively,⁴⁰ and since peptoid sequences can be deduced sensitively by Edman degradation⁴¹ or mass spectrometry,⁴² encoding strategies are not required to identify hits in binding screens. Moreover, peptoids are protease-insensitive, an attribute critical to their potential use as antibody surrogates.¹³

- (30) Hurwitz, H.; Fehrenbacher, L.; Novotny, W.; Cartwright, T.; Hainsworth, J.; Heim, W.; Berlin, J.; Baron, A.; Griffing, S.; Holmgren, E.; Ferrara, N.; Fyfe, G.; Rogers, B.; Ross, R.; Kabbinavar, F. *New Engl. J. Med.* **2004**, *350*, 2335–2342.
- (31) Johnson, D. H.; Fehrenbacher, L.; Novotny, W. F.; Herbst, R. S.; Nemunaitis, J. J.; Jablons, D. M.; Langer, C. J.; DeVore, R. F., III; Gaudreault, J.; Damico, L. A.; Holmgren, E.; Kabbinavar, F. *J. Clin. Oncol.* **2004**, *22*, 2184–2191.
- (32) Ambresin, A.; Mantel, I. *Rev. Med. Suisse* **2007**, *3*, 137–141.
- (33) Brekken, R. A.; Overholser, J. P.; Stastny, V. A.; Waltenberger, J.; Minna, J. D.; Thorpe, P. E. *Cancer Res.* **2000**, *60*, 5117–5124.
- (34) Kim, K. J.; Li, B.; Winer, J.; Armanini, M.; Gillett, N.; Phillips, H. S.; Ferrara, N. *Nature* **1993**, *362*, 841–844.
- (35) Prewett, M.; Huber, J.; Li, Y.; Santiago, A.; O'Connor, W.; King, K.; Overholser, J.; Hooper, A.; Pytowski, B.; Witte, L.; Bohlen, P.; Hicklin, D. J. *Cancer Res.* **1999**, *59*, 5209–5218.
- (36) Getmanova, E. V.; Chen, Y.; Bloom, L.; Gokemeijer, J.; Shamah, S.; Warikoo, V.; Wang, J.; Ling, V.; Sun, L. *Chem. Biol.* **2006**, *13*, 549–556.
- (37) Motzer, R. J.; Michaelson, M. D.; Redman, B. G.; Hudes, G. R.; Wilding, G.; Figlin, R. A.; Ginsberg, M. S.; Kim, S. T.; Baum, C. M.; DePrimo, S. E.; Li, J. Z.; Bello, C. L.; Theuer, C. P.; George, D. J.; Rini, B. I. *J. Clin. Oncol.* **2006**, *24*, 16–24.
- (38) Clark, J. W.; Eder, J. P.; Ryan, D.; Lathia, C.; Lenz, H. J. *Clin. Cancer Res.* **2005**, *11*, 5472–5480.
- (39) Fabiano, M. A.; Biggs, W. H., 3rd; Treiber, D. K.; Atteridge, C. E.; Azimioara, M. D.; Benedetti, M. G.; Carter, T. A.; Ciceri, P.; Edeen, P. T.; Floyd, M.; Ford, J. M.; Galvin, M.; Gerlach, J. L.; Grotzfeld, R. M.; Herrgard, S.; Insko, D. E.; Insko, M. A.; Lai, A. G.; Lelias, J. M.; Mehta, S. A.; Milanov, Z. V.; Velasco, A. M.; Wodicka, L. M.; Patel, H. K.; Zarrinkar, P. P.; Lockhart, D. J. *Nat. Biotechnol.* **2005**, *23*, 329–336.
- (40) Figliozzi, G. M.; Goldsmith, R.; Ng, S. C.; Banville, S. C.; Zuckermann, R. N. *Methods Enzymol.* **1996**, *267*, 437–447.
- (41) Alluri, P. G.; Reddy, M. M.; Bacchawat-Sikder, K.; Olivos, H. J.; Kodadek, T. *J. Am. Chem. Soc.* **2003**, *125*, 13995–14004.
- (42) Paulick, M. G.; Hart, K. M.; Brinner, K. M.; Tjandra, M.; Charych, D. H.; Zuckermann, R. N. *J. Comb. Chem.* **2006**, *8*, 417–426.

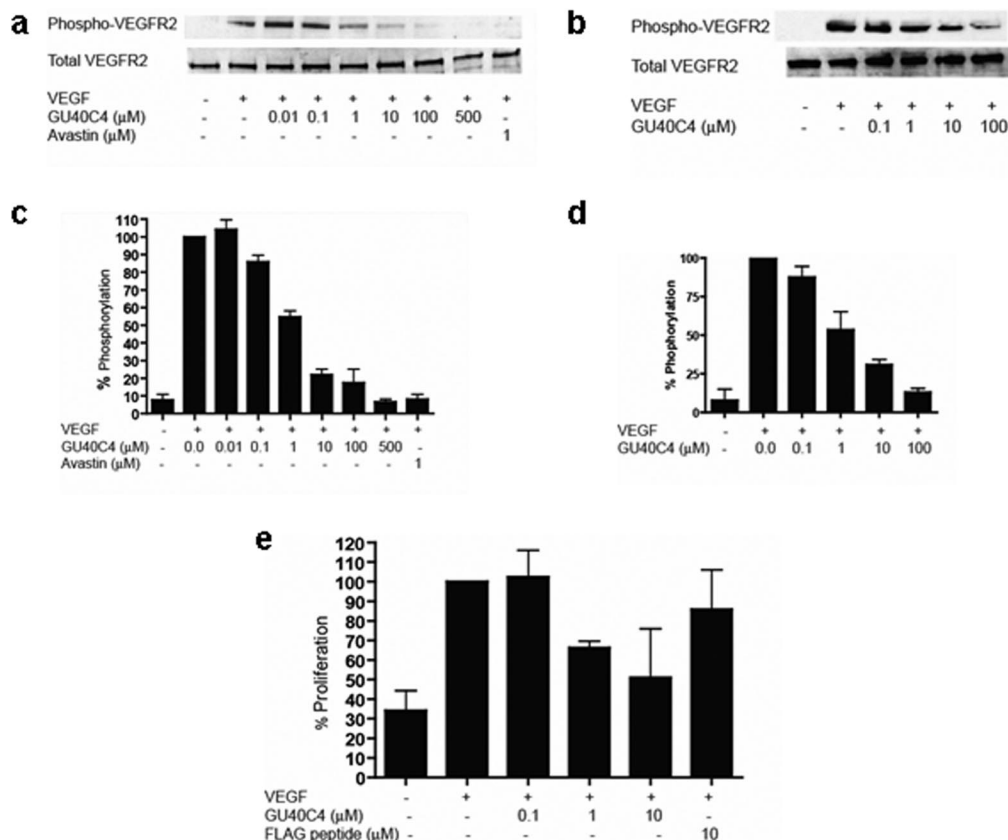


Figure 5. Effects of GU40C4 on VEGF-induced VEGFR2 activity in cultured cells. (a) Effect of the indicated levels of GU40C4 and Avastin on phosphorylation of VEGFR2 in PAE/KDR cells after treatment with VEGF (1.3 nM) for 7 min. Phosphorylated VEGFR2 and total VEGFR2 were visualized by Western blotting cell lysates with antibodies specific for VEGFR2 and phosphorylated VEGFR2. (b) The same experiment described in (a) but conducted on HUVEC cells. (c, d) Quantification of the data shown in (a,b) reveal an IC_{50} value of approximately 1 μ M. (e) Quantification of HUVEC proliferation in the absence and presence of VEGF (1.3 nM) and \pm GU40C4. After 4 days, viable cells were determined using a luminescent assay. GU40C4 inhibited VEGF-induced HUVEC proliferation by 50% at 1 μ M and almost completely at 10 μ M. FLAG peptide had no effect on HUVEC proliferation at 10 μ M.

We have previously established conditions to screen bead-displayed peptoid libraries for ligands to well-behaved, soluble proteins.¹⁶ However, integral membrane receptors such as VEGFR2 do not generally display such favorable biochemical characteristics. Therefore, we developed a two-color, cell-based screen (Figure 1a) that allows the receptor to be displayed in a relatively natural cellular environment. It is important to point out that this is not the first study to employ cells in a bead-based screen. In particular, the elegant work of Lam and co-workers¹⁹ is noteworthy. They reported a screen of an encoded bead-based library of peptidomimetic compounds against $\alpha_4\beta_1$ integrin that employed integrin-expressing Jurkat cells and on several other receptor targets.⁴ Nonetheless, the two-color technology reported here represents an advance in cell-based screening technology in that it eliminates the requirement for subtractive screening or for a known receptor–ligand to be employed as a competitor⁴⁴ and makes it relatively easy to identify ligands for the specific receptor of interest. The use of parental cell line that lacks the receptor of interest and is labeled with a quantum dot of a different color than that used to label the receptor-expressing cells is critical for allowing the facile identification of the extremely rare hits in these large combinatorial libraries. In this present study, only five of the approximately 300 000 beads screened (approximately 0.0017% of the population) were observed to bind PAE/KDR (red-stained) cells only (Figure 1d). It would have been exceedingly difficult to identify the beads that display these rare peptoids without the high contrast provided by the particular two-color

assay that we report here. Another distinguishing feature of this work compared to earlier work is the use of quantum dot labels rather than organic fluorophores. The large Stokes shifts of the quantum dots overcome the relatively high autofluorescent background emission of the beads when they are irradiated with UV light.⁴³ Also, the quantum dot products used penetrate into the cells, thus avoiding significant modification of the cell surface.

Of course, many cell-based assays have been reported in which activation of a downstream reporter gene, or some other easily monitored event, is triggered by a small molecule, but these assays require spatial separation of the cells and molecules into different wells of a microtiter plate and thus a significant robotics infrastructure to carry out screens of large numbers of compounds. Furthermore, it is always possible to isolate molecules that modulate the reporter event in some way other than by binding to the receptor. In contrast, our screen registers only selective binding to the target receptor and requires no specialized equipment other than a fluorescence microscope and can easily accommodate libraries containing hundreds of thousands of molecules.

The power of this approach was displayed in this study, which resulted in the isolation of modest affinity VEGFR2 ligands that were elaborated into high affinity binders through dimerization.

(43) Olivos, H. J.; Bachhawat-Sikder, K.; Kodadek, T. *ChemBiochem* **2003**, *4*, 1242–1245.

(44) Liang, W. C.; Wu, X.; Peale, F. V.; Lee, C. V.; Meng, Y. G.; Gutierrez, J.; Fu, L.; Malik, A. K.; Gerber, H. P.; Ferrara, N.; Fuh, G. *J. Biol. Chem.* **2006**, *281*, 951–961.

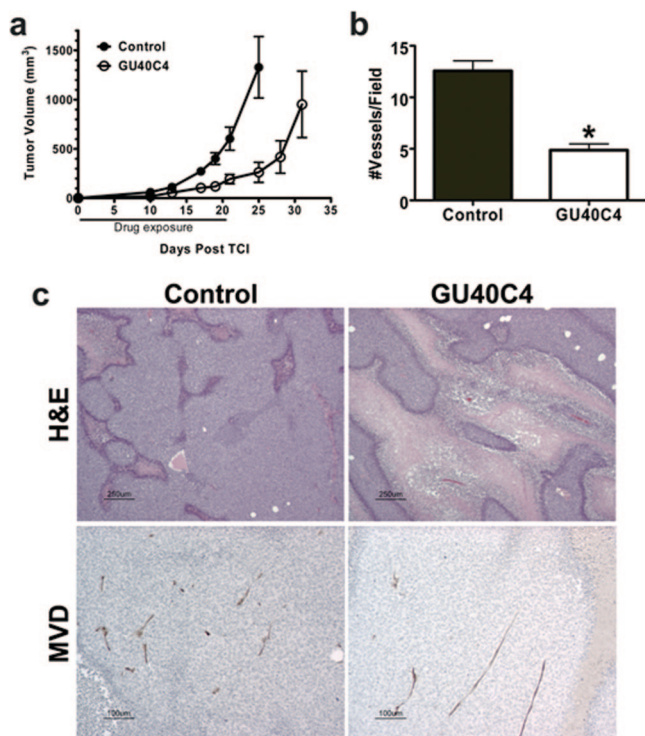


Figure 6. GU40C4 blocks tumor angiogenesis in vivo; 2.5 million A673 cells (human Ewings' sarcoma) were injected into the right flank of female nude mice on Day 0. Also on Day 0, Alzet pumps loaded with 800 μg of GU40C4 ($n = 10$) or a control peptide ($n = 11$) were implanted subcutaneously at a distant site. The pumps elute for approximately 21 days. (a) Tumor growth was reduced during the course of treatment in GU40C4 animals compared to control ($p < 0.001$ on day 19, 21 by two-way ANOVA). (b) Microvessel density, as determined by CD34 staining on tissue from animals sacrificed on day 22, was significantly reduced in GU40C4-treated animals ($p < 0.0001$) compared to control. (c) H&E sections from control and treated animals reveals tumor necrosis associated with GU40C4 treatment (top panels) and representative samples of CD34 staining (bottom panels).

The GU40C4 peptide was shown to bind VEGFR2 with a K_D of between 20 and 30 nM (Figure 3 and Supplementary Figure 7) and was found to be a fairly potent antagonist of VEGF-activated VEGFR2 function in vitro (Figure 5 and Supplementary Figure 8). More importantly, GU40C4 displayed antiangiogenic activity in an A673 tumor xenograft model that has been used extensively for evaluation of anti-VEGF strategies for cancer therapy.^{44,45} The peptide had a potent therapeutic effect in vivo with no apparent adverse effects to normal tissue at a modest dose (800 μg delivered to an ~ 20 g mouse over 21 days). This dose of 1.9 mg/kg/day compares very favorably with that required for low molecular weight tyrosine kinase inhibitors that have activity against VEGFR2. For instance, Sutent and Nexavar are effective at controlling tumor growth and angiogenesis at doses of 40 and 30 mg/kg/day, respectively.^{46,47} The nearly 8 days of tumor growth delay following cessation of peptide therapy (Figure 6a) suggests that the serum half-life is

higher than one might expect of the 2.8 kD GU40C4 (about 1.9% the mass of an IgG). This could be due in part to binding of plasma proteins or retention and pooling of GU40C4 in the tumor microenvironment, though a definitive answer must await detailed pharmacokinetic analysis. In any case, the serum stability of peptoids is a clear advantage over peptide-based drug candidates that are sensitive to protease-mediated degradation. Furthermore, the small size of GU40C4 may aid in tumor penetration and binding of VEGFR2, which is predominately located on the abluminal surface of endothelial cells. The 50% inhibition of microvessel density (Figure 6b) induced by GU40C4 at the end of therapy is consistent with blockade of VEGFR2 activity with other VEGFR2 antagonists, such as DC101, a rat monoclonal anti-mouse VEGFR2 antibody.²¹ Overall, these in vivo data strongly support further development of GU40C4 and other peptoid-based therapeutics for antiangiogenic therapy as well as the application of this technology platform to the isolation of peptoid agonists or antagonists of other clinically interesting cell surface receptors.

Experimental Section

Two-Color On-Bead Cell Screening Assay. For each of the three rounds of the experiment, about 100 000 beads were allowed to swell in DMF, washed with PBS, and finally equilibrated in 3% BSA containing DMEM media for 1 h. PAE/KDR and PAE parental cells (Sibtech, Inc.) were removed from culture plates using enzyme-free cell dissociation buffer (Gibco), washed, and resuspended in DMEM media. Cells were labeled using quantum dots (Invitrogen) following the manufacturer's protocol. PAE/KDR cells labeled with Qtracker 655 (red) and PAE parental cells labeled with Qtracker 565 (green). Both labeled cells were mixed in a 1:1 ratio, using approximately 1×10^6 of each cell type, and gently stirred to break cell clusters. The cell suspension was then added to culture plates containing the beads and incubated at 37 $^\circ\text{C}$ with gentle shaking for 60–75 min. The beads were gently washed two times with DMEM media and visualized under the fluorescent microscope (Olympus BX-51) equipped with a DAPI filter (100 \times total magnification). Individual beads containing fluorescently tagged red cells only were collected manually with a 20 μL pipet using medium size pipet tips. Selected beads were washed and boiled with 1% SDS solution for 30 min to strip off cells and other debris, then subjected to automated Edman sequencing.

Peptoid Library Design and Synthesis. The design of the library (Figure 1b) took in to account the structure of the VEGF–VEGFR2 complex. The extracellular domain of the receptor consists of seven extracellular immunoglobulin (Ig)-like domains.²³ VEGF binds to Ig domains 2 and 3.²³ It has been reported that isoleucine (Ile-43, 46, 83), glutamate (Glu-64), phenylalanine (Phe-17), glutamine (Gln-79), lysine (Lys-84), and proline (Pro-85) side chains of VEGF are important moieties for binding to VEGFR2.⁴⁸ Therefore, in designing our peptoid library, we selected Lys-like and Leu-like residues to be fixed at the C-terminus of each molecule in the library with the intent of biasing the library for VEGFR2 binding. Leu was chosen instead of Ile because Ile was not validated for peptoid synthesis at the time of synthesis. Also, we decided to place one additional Lys-like residue between the resin and the 8-mer peptoid, making the full length of each peptoid nine residues. The positively charged Lys-like residue repels the peptoids from each other on the bead surface and helps avoid peptoid aggregation.

(45) Rad, F. H.; Le Buanec, H.; Paturance, S.; Larcier, P.; Genne, P.; Ryyffel, B.; Bensussan, A.; Bizzini, B.; Gallo, R. C.; Zagury, D.; Uzan, G. *Proc. Natl. Acad. Sci. U.S.A.* **2007**, *104*, 2837–2842.

(46) Wilhelm, S. M.; Carter, C.; Tang, L.; Wilkie, D.; McNabola, A.; Rong, H.; Chen, C.; Zhang, X.; Vincent, P.; McHugh, M.; Cao, Y.; Shujath, J.; Gawlak, S.; Eveleigh, D.; Rowley, B.; Liu, L.; Adnane, L.; Lynch, M.; Auclair, D.; Taylor, I.; Gedrich, R.; Voznesensky, A.; Riedl, B.; Post, L. E.; Bollag, G.; Trail, P. A. *Cancer Res.* **2004**, *64*, 7099–7109.

(47) Mendel, D. B.; Laird, A. D.; Xin, X.; Louie, S. G.; Christensen, J. G.; Li, G.; Schreck, R. E.; Abrams, T. J.; Ngai, T. J.; Lee, L. B.; Murray, L. J.; Carver, J.; Chan, E.; Moss, K. G.; Haznedar, J. O.; Sukbuntherng, J.; Blake, R. A.; Sun, L.; Tang, C.; Miller, T.; Shirazian, S.; McMahon, G.; Cherrington, J. M. *Clin. Cancer Res.* **2003**, *9*, 327–337.

(48) Muller, Y. A.; Li, B.; Christinger, H. W.; Wells, J. A.; Cunningham, B. C.; de Vos, A. M. *Proc. Natl. Acad. Sci. U.S.A.* **1997**, *94*, 7192–7197.

The library was synthesized on TentaGel macrobeads (140–170 μM diameter), which have excellent stability and swelling properties and also provide a nonsticky surface that is ideal for reducing nonspecific binding in screening experiments.¹¹ Synthesis of the library was conducted using eight different amines (Figure 1b), resulting in a theoretical diversity of 262 144 compounds.

The 9-mer peptoid library was synthesized on TentaGel macrobeads (140–170 μm ; substitution: 0.48 mmol/g resin; Rapp Polymer) using a microwave (1000 W)-assisted synthesis protocol. TentaGel macrobeads were distributed equally into eight peptide synthesis reaction vessels and swelled in dimethylformamide (DMF); each reaction vessel was treated with 2 M bromoacetic acid and 3.2 M diisopropylcarbodiimide (DIC), and the coupling was performed in a microwave oven set to deliver 10% power (2 \times 15 s). After washing the beads with DMF, each vessel was treated with one of the eight primary amines at 2 M concentration, and again, the coupling was performed in the microwave oven as described above. The beads were washed, pooled, randomized, and redistributed equally into eight peptide synthesis vessels, and the procedure was repeated until the desired length was achieved. For the first three fixed residues (Nleu-Nlys-Nlys), each step was followed as above except the pooling step. At the completion of the library synthesis, beads were treated with a 95% TFA, 2.5% triisopropylsilane, and 2.5% water mixture for 2 h to remove side chain protection groups and were neutralized with 10% diisopropylethylamine in DMF. Finally, the beads were washed with dichloromethane, dried, and stored at 4 $^{\circ}\text{C}$.

Dimeric Library Synthesis. The dimer libraries were synthesized on Knorr amide MBHA resin (substitution: 0.78 mmol/g resin; Novabiochem). First, Fmoc-Cys(Trt)-OH was loaded onto the bead (HOBt, HBTU, DIPEA) followed by Fmoc-Lys(Dde)-OH (HOBt, DIC). Then the Fmoc group was selectively removed and coupled different numbers and combinations of Fmoc- β -Ala-OH or/and Fmoc- ϵ -Ahx-OH (HOBt, DIC) onto the N-terminal amino group of Lys in longer dimer series. Then, both the Fmoc and Dde groups were removed (2% hydrazine and 20% piperidine) and continued general microwave-assisted peptoid synthesis steps as described in the library synthesis procedure until the total nine residues were added. Here in each treatment, the residues were added to both open amine ends (double addition) ultimately connected via Lys to the resin. In shorter dimers, after coupling with initial Cys, Fmoc-Lys(Fmoc)-OH was coupled. Once both Fmoc groups were removed simultaneously, direct coupling of peptoid residues (avoiding linker region) was conducted again using the microwave-assisted protocol, which resulted in double addition as described above. Also for these truncated peptoid dimers, we avoided adding C-terminal residues one at a time up to the first three residues, which ultimately resulted shorter dimers with 6–8 residues in each monomer unit. After the synthesis, peptoid dimers were cleaved off the resin using 95% TFA, 2.5% triisopropylsilane, and 2.5% water mixture for 2 h and purified using HPLC. Each compound was treated with fluorescein-5-maleimide (pH = 7; Pierce) in PBS to attach the FITC group and were repurified using HPLC.

Resynthesis of Biotinylated and FITC-Labeled Peptoids. In both monomeric and dimeric forms, resynthesis of peptoid ligands was conducted on Knorr amide MBHA resin. After loading a Cys residue, the general microwave-assisted protocol was used to build the peptoid portion and finally fluorescein-5-maleimide or maleimide PEO₂-biotin (Pierce) was coupled.

ELISA-Based Binding Assay. White, clear bottom 96-well plates (Corning Inc.) were coated with 1 $\mu\text{g}/\text{mL}$ recombinant human VEGFR2 protein (R&D Systems) using the sensitizing buffer (0.621 g of NaHCO₃ and 0.275 g of Na₂CO₃ dissolved on 100 mL of ddH₂O, pH = 9.5) overnight at 4 $^{\circ}\text{C}$. The solution was washed with 3 \times 200 μL of wash buffer (1 \times PBS with 0.05% Tween-20) and blocked with Startingblock block buffer (Pierce). Fifty microliters of serial dilutions of FITC-labeled peptoids dissolved in Startingblock block buffer was added to each well and allowed to react for 1 h at room temperature. Wells were washed

with 5 \times 200 μL of wash buffer, and remaining fluorescence was measured at 520 nm using a plate reader (Fluostar Optima, BMG Laboratories, Durham, NC). For competition assays, serial dilutions of unlabeled peptoids were mixed with constant amounts of FITC-labeled peptoids.

Fluorescence Polarization Based Binding Assay. The fluoresceinated GU40C4 (5 nM) was incubated with concentration gradient (0.5 μM to 10 pM) of VEGFR2 in 0.1% BSA in PBS (1 \times , pH 7.4) in a final volume of 100 μL at room temperature for 1–2 h in the dark. The fluorescence polarization values were then measured on a Panvera Beacon 2000 instrument (Invitrogen).

GU40C4 Cell Surface Binding Assay. Different types of cells (PAE/KDR, PAE/Flt-1, PAE, HUVEC, HeLa, HEK-293, MCF-7, HFF) were grown overnight on each well of chamber slides (Nalge Nunc International) (20 000 cells/chamber) coated with gelatin. The cells were washed with PBS, and each chamber was treated (except the control) with 75 nM biotinylated GU40C4 peptoid in PBS for 30 min at 4 $^{\circ}\text{C}$. After washing with PBS, bound biotinylated GU40C4 was probed with Qdot 655 streptavidin conjugate (Invitrogen) treatment for 30 min at 4 $^{\circ}\text{C}$. After the final washing, cells were mounted by ProLong Gold antifade reagent with DAPI (Invitrogen) and visualized under DAPI filter of the fluorescence microscope at 400 \times total magnification (Olympus BX-51).

Western Blots. Experiments were conducted using PAE/KDR and HUVEC that were grown on 6-well plates. Cells were serum starved overnight and treated with different concentrations of GU40C4 peptoid for 15 min followed by 1.3 nM VEGF for 7 min (Invitrogen) or Avastin (Genentech) treated VEGF at 37 $^{\circ}\text{C}$. Cells were treated with nuclear lysis buffer, and lysates were separated by SDS-PAGE and transferred to PVDF membranes. Membranes were probed with antiphospho-VEGF receptor 2 (Tyr1175, 19A10) or total anti-VEGFR2 primary antibodies (Cell Signaling Technology, Danvers, MA) and subsequently developed with appropriate HRP-conjugated secondary antibody (BioRad) followed by enhanced chemiluminescent detection (Pierce).

HUVEC Proliferation Assay. HUVEC cells (ScienceCell) were harvested using enzyme-free cell dissociation buffer and resuspended in endothelial cell media (ECM) with 5% FBS. Cells were plated (2000 cells/well) on white, clear bottom 96-well plates coated with gelatin. After 24 h, the serum was reduced to 0.2% FBS and VEGF (1.3 nM) in the presence or absence of GU40C4 peptoid or FLAG peptide was added. After an additional 2 days, the treatment was repeated with fresh media (0.2% FBS) and reagents. After 4 days, viable cells were determined using CellTiter-Glo Luminescent Cell Viability Assay Kit (Promega, Madison, WI) using a plate reader (BMG Laboratories).

HUVEC Tube Formation Assay. Endothelial cell medium gel (ECM gel) was thawed overnight at 4 $^{\circ}\text{C}$, and 50 μL was added to each well of a prechilled white, clear bottom 96-well plate and incubated for 30 min to facilitate formation of a three-dimensional matrix. HUVECs were harvested using enzyme-free cell dissociation buffer and resuspended in ECM with 0.2% FBS and treated with 1.3 nM VEGF and different concentrations of GU40C4 peptoid, 10 μM control peptoid, GU40C (monomer) or GU40CC (ineffective dimer); 150 μL of treated cell suspension (20 000 cells) was added per well and incubated at 37 $^{\circ}\text{C}$ and visualized tube formation under the light microscope after 16 h (100 \times total magnification). Quantification was conducted as follows: Number of connected cells were divided by total number of cells in the same field to give % tube formation,⁴⁹ and the data obtained in each experiment were further corrected to a % by converting VEGF only induced panel to 100%.

Cell Culture. The human Ewing's sarcoma cell line A673⁵⁰ (CRL-1598, ATCC, Manassas, VA) was grown as a monolayer in

(49) Jung, H. J.; Shim, J. S.; Lee, H. B.; Kim, C. J.; Kuwano, T.; Ono, M.; Kwon, H. J. *Biochem. Biophys. Res. Commun.* **2007**, *353*, 376–380.

(50) Martinez-Ramirez, A.; Rodriguez-Perales, S.; Melendez, B.; Martinez-Delgado, B.; Urioste, M.; Cigudosa, J. C.; Benitez, J. *Cancer Genet. Cytogenet.* **2003**, *141*, 138–142.

Dulbecco's minimal essential medium (Invitrogen, Carlsbad, CA) supplemented with 10% heat-inactivated fetal calf serum (Atlanta Biologicals, Lawrenceville, GA). Cells were maintained at 37 °C in a mixture of 5% CO₂ and 95% air. Cell viability was monitored by Trypan Blue (Invitrogen, Carlsbad, CA) exclusion after trypsinization. Cell fingerprinting was performed by Dr. Luc Girard at the McDermott Center at UT Southwestern to verify identity of cells, and the cells were also tested and found to be negative for mycoplasma prior to use.

In Vivo Activity of GU40C4. Tumors were established in the right flank of 6–8 week old female athymic *nu/nu* mice (NCI, Frederick, MD) by subcutaneous injection of 2.5 million cells in a volume of 50 μ L of PBS. On the same day, an Alzet subcutaneous pump (DURECT Corporation, Cupertino CA) was implanted per manufacturer's recommendations. Briefly, the pumps were filled with 100 μ L of GU40C4 or control peptoid (8 mg/mL in saline). Pumps were weighed empty and again when filled to ensure correct loading. On the basis of the mean pumping rate (0.2 μ L/h), these pumps were predicted to elute for 21 days. Implantation of the pump was performed by making a small incision on the back of the anesthetized animal and subsequently using a hemostat to create a subcutaneous pocket in which to place the pump. The incision was closed with a 5-0 prolene (Ethicon, Somerville, NJ). Animal weights and tumor volumes (calipers) were recorded twice weekly. Volumes were calculated using the formula $D \times d^2 \times 0.52$, where D is the long diameter and d is the perpendicular short diameter. All animal experiments were approved by and performed in accordance with the Institutional Animal Care and Use Committee of UT Southwestern.

Immunohistochemistry. Formalin-fixed tissues were embedded in paraffin, sectioned, and stained with hematoxylin and eosin by the Molecular Histopathology Laboratory at UT Southwestern. H&E photographs were taken at a total magnification of 40 \times on a Nikon DXM 1200 digital camera (Melville, NY). For immunohistochemical staining, slides were deparaffinized by heating at 60 °C for 1 h followed by immersion in xylenes. Tissue was rehydrated by sequential immersion in ethanols. Endogenous peroxidase activity was blocked with 3% H₂O₂ in methanol. Antigen retrieval was performed using pH 6.0 citrate buffer (LabVision, Fremont, CA) for 15 min in a pressure cooker. Sections were blocked with 20%

Aquablock (EastCoast Bio, North Berwick, ME) and subsequently incubated overnight at 4 °C with 1:25 dilution of rat antimouse CD34 (ab8158, Abcam, Cambridge, MA). The primary antibody was detected by incubating with a biotinylated donkey antirat IgG (Jackson ImmunoResearch, Westgrove, PA) followed by the ABC detection kit (Vector Laboratories, Burlingame, CA). Subsequent DAB (Invitrogen, Carlsbad, CA) detection was performed, and slides were counterstained with hematoxylin (Richard Allan Scientific, Kalamazoo, MI) and mounted with Crystal/Mount (Biomedex, Foster City, CA). Microvessel density (MVD) was determined by manually counting the number of blood vessels visible in the microscopic field of view (total magnification, 100 \times). Five fields were taken for each slide ($n = 3$ per group).

Acknowledgment. We thank Dr. David Chen (UTSW) for providing access to a fluorescence microscope, and Dr. Debabrata Saha (UTSW) for light microscopic images. This work was supported by a contract from the National Heart, Lung, and Blood Institute (NO1-HV-28185) for the UT Southwestern Center for Proteomics Research, a grant from the Welch Foundation (I-1299), a postdoctoral fellowship from The Susan G. Komen Foundation, and the Effie Marie Cain Scholarship for Angiogenesis Research.

Supporting Information Available: Peptoid synthesis outline, chemical structures of three additional hits identified from the library screen, dimeric peptoid library binding study results, structures of control compounds used, Western blot analysis of monomers affecting on VEGF-induced VEGFR2 phosphorylation, binding isotherm of GU40C4 against VEGFR2 derived from fluorescence polarization, binding isotherms of GU40C4 against VEGFR1 derived from ELISA studies, HUVEC tube formation assay results, quantifications of HUVEC tube formation assay, and MALDI-MS data. This material is available free of charge via the Internet at <http://pubs.acs.org>.

JA711193X